Advanced Research in Electrical and Electronic Engineering
p-ISSN: 2349-5804; e-ISSN: 2349-5812 Volume 5, Issue 1 January-March, 2018, pp. 50-55
© Krishi Sanskriti Publications
http://www.krishisanskriti.org/Publication.html

THEORETICAL STUDY OF CARRIER TRANSPORT IN CYLINDRICAL GATE-ALL-AROUND SILICON NANOWIRE MOSFET

Lalit Singh[1], Mahesh Chandra[2] and B P Tyagi[3]

[1]Govt. Degree College Jainti, Almora, UK, India
[2, 3]DBS (PG) College Dehradun, UK, India

Abstract—*This paper summarizes some of the essential aspects of carrier transport in Silicon nanowire Cylindrical Gate-All-Around MOSFET. For this, Self consistent solution of the 2-D Schrodinger equation and the 3-D Poisson equation in cylindrical coordinate system, coupled with the drift-diffusion transport equation is discussed. The details of the discretization of these equations and overall steps used to obtain the drain current of the presented device are computed. Simulated drain current versus gate voltage characteristics have also been successfully examined and matched with the data available in the recent literature. Variation of the drain current as a function of the nanowire diameter and of the channel length and is examined. The device performances in terms of off-state current, threshold voltage and parasitic short-channel effects are also computed. It is observed that quantum-mechanical confinement is very important in cylindrical nanowires, which reduces the impact of parasitic short-channel effects.*

Keywords*: Nanowire, Drift-Diffusion Transport, MOSFET, Short-channel effects.*

1. INTRODUCTION

Currently the Modeling and simulation of nanowire MOSFETs devices are experiencing a growing interest due to their unique capabilities: (i) it provides useful insights into device operation since all internal physical quantities that cannot be measured on real devices are available as outputs; (ii) the predictive capability of simulation studies makes possible the reduction of systematically experimental investigation of these new ultra-scaled devices; (iii) It offers the possibility to test hypothetical devices which have not yet been manufactured. Now a day's computers are easily available resources, it (simulation) is becoming a prominent tool for the device physicist, not only for the device optimization, but also for important studies of several peculiar phenomenon in ultra-short channel devices (quantum confinement of charge carriers or short-channel electrostatic effects)[2, 3,7,9-14,18-20].

This study presents a theoretical study of electrostatics and electronic transport in Gate all around nanowire MOSFETs by quantum drift-diffusion numerical simulation. We discussed the operation of presented device using a 2-D/3-D Schrodinger/Poisson solver (MuGFET simulator). MuGFET also provides a lot of information and valuable physical insights (such as the 3-D profile of electrostatic potential, classical and quantum carrier densities in the channel, the energy levels and total inversion charge) used to investigate the influence of short-channel and quantum-mechanical effects [9, 11-12].

2. THEORETICAL BACKGROUND OF THE SIMULATION:

This is based on the numerical solving of the Poisson-Schrodinger equations coupled with the drift-diffusion equation [2,-8]. Here, the Poisson equation is solved on the entire 3-D structure [13] and to solve the Schrodinger equation device is divided into parallel vertical slices (y-z plane) [14]. In order to obtain the wave function, the quantum energy levels and the charge density, in each slice the 2-D Schrödinger equation is thoroughly discussed. To make easy calculations, in radially-symmetric nanowire, it is possible to reduce the size of the Poisson and Schrödinger equations. By expressing these equations in cylindrical coordinates and using the property of cylindrical symmetry of the structure, the Poisson equation reduces into a 2-D equation and the Schrödinger equation becomes 1-D. In this structure (Cylindrical nanowire MOSFETs), the Cartesian coordinates are transformed in cylindrical coordinates (for GAA structure), in such a way that the structure is symmetrical with respect to the coordinate θ. The Poisson equation is solved in two dimensions, on the 2-D mesh as θ is ignored. In the same way, the circular symmetry allows us to simplify the Schrödinger equation along the radial direction r (1-D mesh). Figure: 1(a) shows the 3-D architecture of the radially-symmetric nanowire MOSFETs considered in the simulation. The device is symmetric with intrinsic thin silicon film and highly doped source and drain ($N_{SD} = 3\times10^{20}$ /cm^3). A midgap metal gates (Φm=4.61 eV) and a 1.05nm thick gate-oxide have been also taken. The gate and the drain biased are at V_G

Table 1: Effective masses & N_{2D}

Material	ml	Mw	mz	nv	N2D
Si(001)/ (100)	0.190	0.190	0.916	2	1.587
	0.190	0.916	0.19	2	3.485
	0.916	0.19	0.19	2	3.485
Si(100)/ (001)	0.19	0.553	0.315	4	5.416
	0.916	0.19	0.19	2	3.485

Figure: 1 - MuGFET simulator (a quantum drift-diffusion simulator) for presented device & (b) simulated electrostatic potential along the y-direction at equilibrium condition (available at www.nanohub.org)

and V_D, and the source is at zero potential respectively.

3. POISSON SOLVER

The general Poisson equation is given by:

$$\frac{\partial^2 V}{\partial r^2}+\frac{\partial^2 V}{r^2\partial\theta^2}+\frac{\partial^2 V}{\partial x^2}=-\frac{\rho(r,x)}{\varepsilon}$$

Here, ε is the permittivity of material used. & ρ is the charge density, having value $q(N_D-n)$

By considering the azimuthal symmetry, this can be written as:

$$\cdot\frac{\partial^2 V}{\partial r^2}+\frac{\partial^2 V}{\partial x^2}=-\frac{\rho(r,x)}{\varepsilon} \quad (1)$$

The solution, using finite difference scheme, of above equation can be written as [15]:

$$\cdot V_{i,j}=\frac{1}{\sum_{i,j}}\left[A_{i,j}+B_{i,j}+\frac{\rho_{i,j}}{\varepsilon_j}\right] \quad (2)$$

Where

$$A_{i,j}=V_{i,j+1}\left(\frac{1}{\Delta r^2}+\frac{1}{r_j 2\Delta r}\right)+V_{i,j-i}\left(\frac{1}{\Delta r^2}-\frac{1}{r_j 2\Delta r}\right)+\frac{V_{i-1,j}+V_{i+1,j}}{\Delta x^2}$$

$$B_{i,j}=\frac{V_{i,j+1}-V_{i,j-1}}{2\Delta r}x\frac{\varepsilon_{j+1}-\varepsilon_{j-1}}{2\Delta r} \quad \&$$

$$\sum_{i,j}=2\left(\frac{1}{\Delta r^2}+\frac{1}{\Delta x^2}\right)$$

Here, i points along the x direction and j points along the r directions of the presented mesh. $\Delta x\ \Delta r$ & are the mesh sizes along x and r axis.

4. SCHRODINGER SOLVER:

In this section we will sove the time independent Schrodinger wave equation with a spatially varying effective mass in cylindrical coordinate system. Which is as follows [16]:

$$-\frac{\hbar^2}{2}\left[\frac{1}{r}\frac{\partial}{\partial r}\left(\frac{1}{m^*}r\frac{\partial}{\partial r}\right)+\frac{\partial}{\partial x}\left(\frac{1}{m^*}\frac{\partial}{\partial x}\right)+\frac{1}{r^2}\frac{\partial}{\partial\theta}\left(\frac{1}{m^*}\frac{\partial}{\partial\theta}\right)\right]\Psi+V_{eff}(r)\Psi=\left[H_{oII}(r)+H_{o\perp}(x)\right]\Psi \quad (3)$$

Here, $V_{eff}(x)$is the effective potential energy profile. i. e. $V_{eff}=V_H+V_{exc.}$ $V_H$is the Hartree self-consistent potential which is nothing but the solution of Poisson equation and V_{exc} is the exchane correlation potential. H_{0II} is the parallel part of H_0, and $H_{o\perp}$ is the transverse part.

For cylindrical symmetry. The solution of equation (3) can be written as

$$\Psi(r,\theta,x)=\Psi(r,x)\frac{1}{\sqrt{\pi}}\exp(ik\theta) \quad (4)$$

Here, $k=\pm1,\pm2,\pm3....$ is the angular quantum number and put the value of Ψ in equation (3), we get

Schrodinger equation along the radial direction that is perpendicular to the x axis is:

$$-\frac{\hbar^2}{2}\left[\frac{1}{r}\frac{\partial}{\partial r}\left(\frac{1}{m^*}r\frac{\partial}{\partial r}\right)+\frac{\partial}{\partial x}\left(\frac{1}{m^*}\frac{\partial}{\partial x}\right)+\frac{1}{m^*}\frac{k^2}{r^2}\right]\Psi(r,x)+V_{eff}(r)\Psi(r,x)=\left[H_{o\perp}(r)+H_{oII}(x)\right]\Psi(r,x)$$

$$-\frac{\hbar^2}{2}\left[\frac{1}{r}\frac{\partial}{\partial r}\left(\frac{1}{m^*}r\frac{\partial}{\partial r}\right)+\frac{1}{m^*}\frac{k^2}{r^2}\right]\Psi(r)+V_{eff}(r)\Psi(r)=H_{o\perp}(r)\Psi(r)\ \text{Or}$$

$$-\frac{\hbar^2}{2}\left[\frac{1}{r}\frac{1}{m^*}\frac{\partial}{\partial r}+\frac{\partial}{\partial r}\left(\frac{1}{m^*}\frac{\partial}{\partial r}\right)+\frac{1}{m^*}\frac{k^2}{r^2}\right]\Psi(r)+V_{eff}(r)\Psi(r)=H_{o\perp}(r)\Psi(r) \quad (5)$$

The radial wavefunction $\Psi(r)$ satisfies the one dimensional Schrodinger equation $H_{o\perp}(r)\Psi(r)=E_m\Psi(r)$under the appropriate boundary conditions. Where E_n is the sub band energy & $\Psi(r)$ is the corresponding wave function. Now by discretization method we will solve equation-5 for different

values of m. For each value of m, a distinct set of wave function and eigen value is obtained. And for all m, the obtained energy levels will be stored and arrange in ascending order from the lowest level to highest level. Similarly the wave function corresponding to each energy level is stored. And now the first lowest level is used to calculate the electron density. This process is executed for both levels. Thus the electron density (n_r) is [17]:

$$n(r) = \sum_{r_1, r_2} g_{r1,r2} \sum_{m}^{N} n_m |\Psi(r)|^2 \tag{6}$$

Here, $g_{r1,r2}$ is the valley degeneracy and equal to 2 for unprimed energy level and 4 for primed level. n_m is the electron density per unit length of m^{th} subband, whose value is: $n_m = N_{1D} \Im_{-1/2}\left(\frac{E_F - E_m}{k_B T}\right)$ (7)

Here, E_F is Quasi-Fermi energy, $\Im_{-1/2}$ is hemi Fermi-Dirac integral [10] and N_{1D} is 1-D effective density of state (1-D DOS) having value

$$N_{1D} = \frac{1}{\pi}\sqrt{\frac{2m_D(r_1, r_2)k_B T}{\hbar^2}} \tag{8}$$

Where $m_D(r_1,r_2)$ is the density of state effective mass and is equal to m_l (longitudinal effective mass) for unprimed energy level and m_t (transverse effective mass) for primed energy level. Finally, the 1-D Schrodinger equation is solved for a vertical cut-line in each mesh point of the x axis. For each cut-line in a given mesh-point i, the electron density n(r) is calculated using equation (6), and then it assigned to the mesh-point point i; this makes possible to build step by step the total density n(x, r). This density gives a new potential V(x, r), and this new potential is again introduced in solving of the Schrodinger equation, which gives the new carrier density n(x, r), which in turn injected into Poisson's equation. This process is going on until the convergence is achieved. This is known as self-consistent method.

5. EXPRESSION OF DRAIN CURRENT:

After solving the Schrodinger and Poisson equations self-consistently, the solutions of these equations are coupled with continuity equation. That is [10]:

J = drift component + diffusion Component

$$J = -q\mu_n n \nabla\phi + qD_n \nabla n \tag{9}$$

Where μ_n is the electron mobility, D_n is the diffusion coefficient, and *n* is the electron density. Poisson, Schrodinger and drift-diffusion equations are solved using a finite difference scheme The expression for ϕ_F, i, j , using discretization of equation-9, is:

$$\phi_{F\ i,j} = \frac{G_{i,j} + C_{i,j}}{\sum_{i,j}} \tag{10}$$

Where

$$C_{i,j} = \frac{\phi_{.fi-1,j} + \phi_{f.i+1,j}}{\Delta x^2} + \phi_{f.i,j-1}\left(\frac{1}{\Delta r^2} - \frac{1}{r_j}\frac{1}{2\Delta r}\right) + \phi_{f.i,j+1}\left(\frac{1}{\Delta r^2} + \frac{1}{r_j}\frac{1}{2\Delta r}\right)$$

$$\sum_{i,j} = 2\left(\frac{1}{\Delta r^2} + \frac{1}{\Delta x^2}\right) \quad \& \quad G_{i,j} = \beta D_{i,j} E_{i,j}$$

$$D_{i,j} = \left[\frac{\phi_{F.i,j+1} - \phi_{F.i,j-1}}{2\Delta x} \cdot \frac{\left(V_{i+1,j} - \phi_{F.i+1,j}\right) - \left(V_{i-1,j} - \phi_{F.i-1,j}\right)}{2\Delta x}\right]$$

$$E_{i,j} = \left[\frac{\phi_{F.i,j+1} - \phi_{F.i,j-1}}{2\Delta r} \cdot \frac{\left(V_{i,j+1} - \phi_{F.i,j+1}\right) - \left(V_{i,j-1} - \phi_{F.i,j-1}\right)}{2\Delta r}\right]$$

Table: 2- Parameters for simulating the presented device by MuGFET (Multigate Field Effect Transistor) simulator.

Material/Band structure	Electrons in channel	Holes in channel	Environment & Biasing
Dielectri constant of channel- 11.7 Dielectric constant of insulator- 4.8 Band gap of channel material- 1.12eV Electron affinity of channel material- 4.05eV Gate contact work function- 4.6eV	Saturation velocity- 1.07e+07cm/sec Minority life time- 500ns Mobility- 1400cm2/Vs Vsat – 1.07e+07cm/sec	Light hole effective mass-0.16 Hevy hole effective mass- 0.49 DOS effective mass- 1.18 Mobility- 450cm2/Vs Vsat – 8.3e+06cm/sec	VG (initial)- 0V VG (final)- 1V VD(initial)- 0V VD(initial)- 0.045 Critical current for Vth–0.0001 (A/um) Maxi no of Newton iterations- 1000. Tolerance for Newtons- 1e-06. Temperature – 300K.

First we calculate ϕ from equation-10, than using Poisson-Schrodinger solver we calculate the carrier density (n). This computed charge density is then used to find a new potential profile, which is then again inserted into the equation for solving the continuity equation that gives new quasi-Fermi energy. This new quasi-Fermi level will be injected into the Schrodinger-Poisson and so on. The process continues until the convergence is achieved. The final values of the electron density, n(x,r), and the quasi- Fermi energy, $\Phi_F(x,r)$, are used for calculating the drain current of the presented device.

$$J_n(x,r) = q\mu_n n(x,r)\nabla\phi_F(x,r) \tag{11}$$

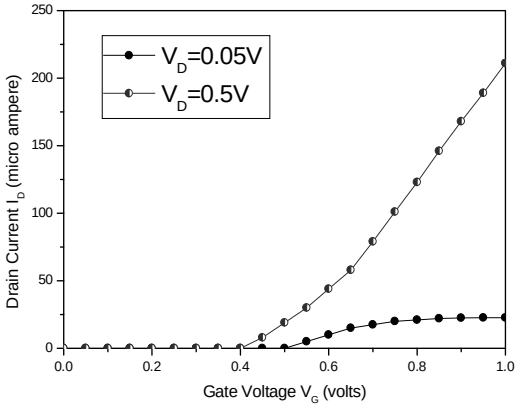

Figure: 2(a)-plot of I_d-V_G (classical drift-diffusion simulation result) for V_D=0.05V & 0.5V.

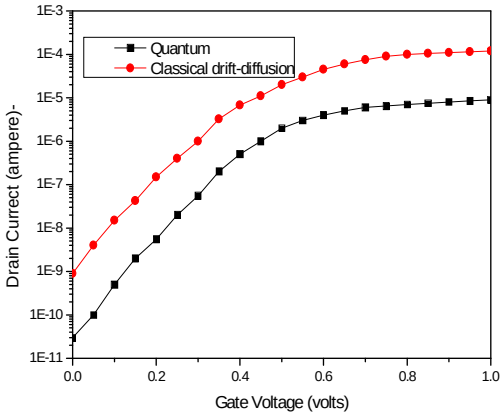

Figure: 2(b)-Variation of drain current with gate voltage for D=L=5nm, at V_D=0.05V

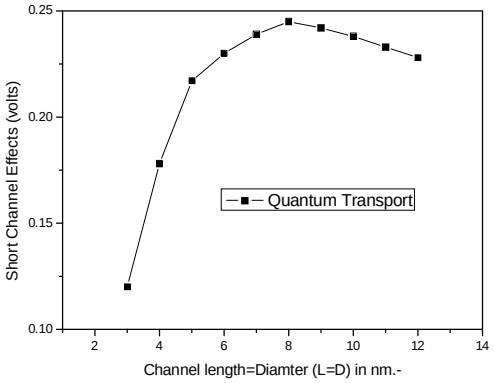

Figure: 2(c)-short channel effects (SCE) versus the nanowire diameter for short-channel devices with L=D.

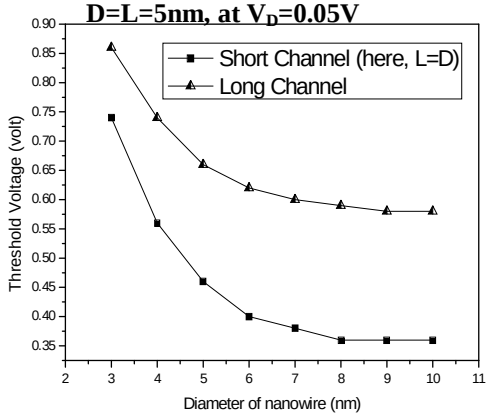

Figure: 2(d)-Threshold voltage versus the nanowire diameter extracted from quantum calculation.

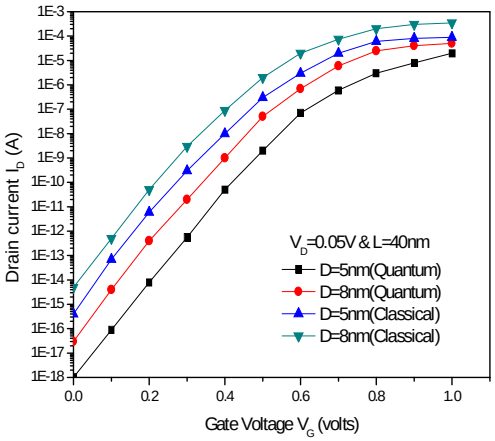

Figure: 2(e) - Plot of drain current as a function of gate voltage for two diameters (D=8 & D=5nm). The length of the device is 40nm and drain bias, V_D=0.05V.

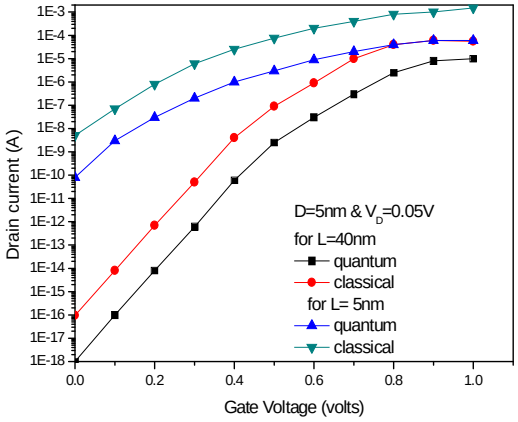

Figure: 2(f) - Plot of drain current as a function of gate voltage for two lengths (L=40 & L=5nm). The diameter of the device is 5nm and drain bias, V_D=0.05V

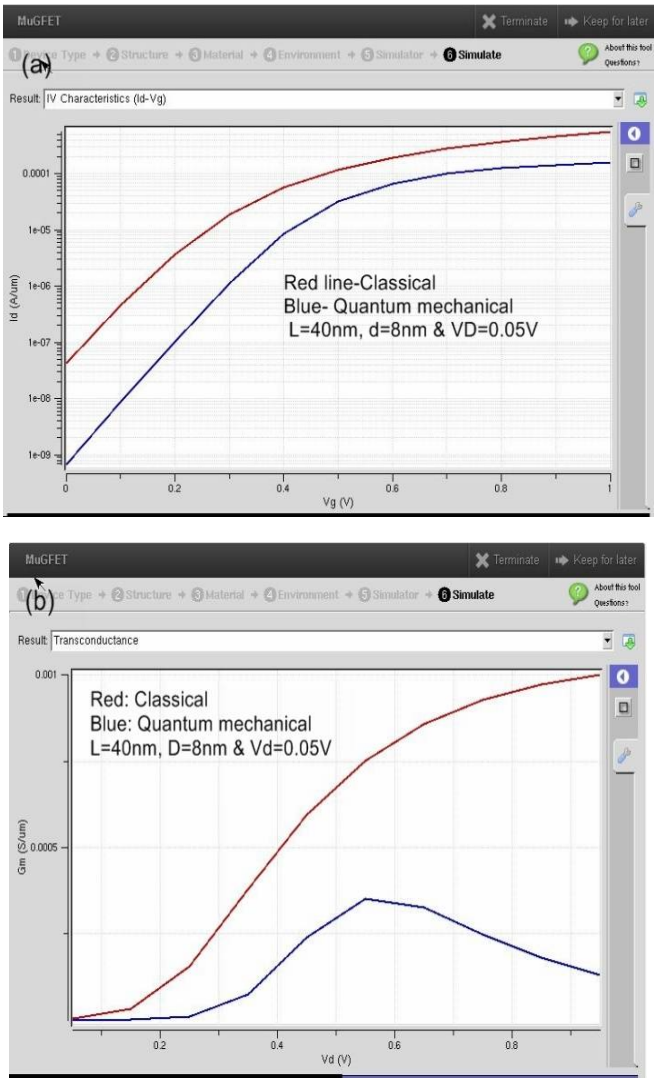

Figure: 3(a) - Simulated I_D-V_G characteristics of presented device by Mu GFET simulator and
(b) - plot of simulated transconductance as a function of drain voltage.

6. RESULT AND DISSCUSSION:

In this study, we mainly focussed on the variation of the drain current as a function of the nanowire diameter and of the channel length and we also discussed the device performances in terms of off-state current, threshold voltage and parasitic short-channel effects.

We start with the variation of the drain current as a function of the nanowire diameter. Figure: 2(e) represents a plot of the drain current characteristics as a function of the gate voltage, as calculated by MuGFET for two diameters 5 nm and 8 nm. Data obtained for both classical and quantum cases are plotted. A first remark concerns the off-state current (i.e., value of the drain current for V_G=0 V). For D=5 nm this current is lower than for D=8 nm, whatever the classical method or quantum. Similarly, the current in the subthreshold regime is lower for the smallest diameter. This is due to the so-called "volume inversion" phenomenon which comes into play in all multiple-gate devices in the sub threshold regime [24]. A second remarkable point, reduction of the drain current in the quantum case as compared to the classical case, for both nanowire diameters presented here. This is due to the existence of a strong "quantum confinement" of carriers leads to the reduction of the charge inversion in the channel, whereas in classical case this effect is not taken into account. Third point to be noted is the difference between the calculated drain current both in classical and quantum case. This difference is larger for D=5 nm than for D=8 nm, as can be seen in Fig. 2(e), particularly in the sub threshold regime. When the nanowire is thinned, the carrier confinement is more dominant and the inversion charge density in the channel reduces. This increases the threshold voltage and leads to a significant decrease of the drain current. Figure: 2(f) shows the variation of the drain current as a function of gate voltage for different channel lengths (for L=40nm & 5nm) and for D=5 nm. In this, we can observe that when the channel length is reduced(for same D) the off-state current strongly increases and the sub threshold slope is much higher than in the case of a long channel (L=40 nm), showing a significant degradation of the device performances. This is because of huge amount of increase in short-channel effects; the gate potential becomes less effective. Thus, parasitic electrostatic affects drastically increase and lead to this large increase in off-state current and sub threshold slope. Such behaviour is observed for both classical or quantum cases. Figure- 2(c) shows the variation of short channel effect (which is equal to the difference between the threshold voltage of the short-channel transistor with L=D and the threshold voltage of the long-channel transistor for a given diameter D) as a function of nanowire diameter for quantum case only. This variation shows that, initially SCS increases up to maximum (at D=8 nm), then it starts to decrease. This is explained by the fact that the strong quantum confinement reduces the short- channel effects. In Figure- 2(d) threshold Voltage as function of the nanowire diameter for a long-channel and short channel (L=D) using quantum mechanical approach is plotted. We note that the threshold voltage of the long channel transistor is higher than that of the short-channel transistor with L=D. This is an expected result because the short channel effects that occur in the transistor with L=D greatly reduces the threshold voltage. One can also note that when the diameter of the nanowire is reduced, the threshold voltage remains constant over a certain range of values and then begin to increase with decreasing the nanowire diameter this increase is because of the quantum confinement of carriers when the diameter is reduced.

REFERENCES

[1] T. Kerkhoven, M. Raschke, and U. Ravaioli, “Self-consistent simulation of quantum wires in periodic heterojunction structures”, Journal of Applied Physics, vol. 74, no. 2, pp. 1199 – 1204, 1993.

[2] J. L. Autran and D. Munteanu, "Simulation of electron transport in nanoscale independent- gate DG devices using a full 2D Green’s function approach", Journal of Computational and Theoretical Nanoscience, vol. 5, pp. 1120–1127, 2008.

[3] C. Raynaud, J.-L. Autran, P. Masson, M. Bidaud and A. Poncet,"Analysis of MOS devices capacitance-voltage characteristics based on the self-consistent solution of the Schrodinger and Poisson equation”, Mat. Res. Soc. Symposium. Proceedings, vol. 592, pp. 159, 2000.

[4] T. Hiramoto, M. Saitoh, G. Tsutsui, “Emerging nanoscale Silicon devices taking advantage of nanostructure physics”, IBM J. Res. Develop., vol. 50, no. 4/5, pp. 411-418, 2006.

[5] J. Martorell, H. Wu, and D. W. L. Sprung, “Systematic trends in self-consistent calculations of linear quantum wires”, Phys. Rev. B, vol. 50, no. 23, pp. 17298-17308, 1994.

[6] T. Kerkhoven, A.T.Galick, U. Ravaioli, J.H. Arends, Y. Saad,“Efficient numerical simulation of electron states in quantum wires”, Journal of Applied Physics, vol. 68, no. 7,pp. 3461-3469,1990.

[7] G. L. Snider, I. H. Tan, and E. L. Hu, “Electron states in mesa-etched one-dimensional quantum well wires”, Journal of Applied Physics, vol. 68, no. 6, pp. 2849 – 2853, 1990.

[8] M. Zervos and L.F. Feiner, "Electronic structure of piezoelectric double-barrier InAs/InP/InAs/InP/InAs (111) nanowires", Journal of Applied Physics, vol. 95, no. 1, pp. 281-291, 0021-8979, 2004.

[9] F. Stern, “Self-consistent results for n-type Si inversion layers”, Phys. Rev. B, vol. 5, p. 4891-4899, 1972.

[10] M. Moreau, D. Munteanu and J.L. Autran, "Simulation Analysis of Quantum Confinement and Short-Channel Effects in Independent Double-Gate Metal-Oxide-Semiconductor Field-Effect Transistors ", Japanese Journal of Applied Physics, vol.47, no. 9, pp. 7013-7018, 2008.

[11] J. S. Blakemore, “Approximations for Fermi–Dirac integrals, especially the function F1/2(ηF) used to describe electron density in a semiconductor,” Solid State Electronics, vol. 25, no. 11, pp. 1067–1076, Nov. 1982.

[12] D. Munteanu, J.L. Autran, X. Loussier, S. Harrison, R. Cerutti, T. Skotnicki, "Quantum Short-Channel Compact Modeling of Drain-Current in Double-Gate MOSFET", Solid State Electronics, vol. 50, no. 4, pp. 630-636, 2006.

[13] D. Munteanu, J.L. Autran, S. Harrison, K. Nehari, O. Tintori, T. Skotnicki, "Compact Model of the Quantum Short-Channel Threshold Voltage in Symmetric Double-Gate MOSFET", Molecular Simulation, vol. 31, no. 12, pp. 831–837, 2005.

[14] C. Raynaud, J.-L. Autran, P. Masson, M. Bidaud and A. Poncet,"Analysis of MOS devices capacitance-voltage characteristics based on the self-consistent solution of the Schrodinger and Poisson equation”, Mat. Res. Soc. Symposium. Proceedings, vol. 592, pp. 159, 2000.

[15] M. Zervos and L.F. Feiner, "Electronic structure of piezoelectric double-barrier InAs/InP/InAs/InP/InAs (111) nanowires", Journal of Applied Physics, vol. 95, no. 1, pp. 281-291, 0021-8979, 2004.

[16] Eric Polizzi and Supriyo Datta, “Multidimensional Nanoscale device modeling: the Finite Element Method applied to the Non-Equilibrium Green’s Function formalism”, School of Electrical and Computer Engineering Purdue University West-Lafayette, Indiana 47907-1285

[17] M. Najmzadeh, J.-M. Sallese, M. Berthomé, W. Grabinski, A.M. Ionescu, “Transport analysis in triangular GAA Si nanowire junction less n MOSFETs”, IEEE Transactions on Electron Devices, 2012,

[18] Dragica Vasileska, Stephen Goodnick (2006). Computational Electronics.

[19] M. P. Anantram1, M. S. Lundstrom2, and D. E. Nikonov, “Modeling of Nanoscale Devices”, Department of Electrical and Computer Engineering, Purdue University, West Lafayette, IN 49097, USA.

[20] Daniela Munteanu and Jean-Luc Autran, “A 2-D/3-D Schrödinger-Poisson Drift-Diffusion Numerical Simulation of Radially-Symmetric Nanowire MOSFETs”, 2012 Munteanu and Autran; licensee In Tech.

[21] Balmos 3D simulation code, L2MP-CNRS (2003).

[22] D. Jimenez, J. J. Saenz, B. Iniguez, Senior Member, IEEE, J. Sune, Senior Member, IEEE, L. F. Marsal, and J. Pallarès, “Modelling of Nanoscale Gate-All-Around MOSFETs”, IEEE Electron Device Letters, Vol. 25, No. 5, Pp-314-16, May 2004.

[23] Christopher P Auth and James D Plummer, “Scaling Theory for Cylindrical Fully-Depleted Surrounding-Gate MOSFET’s”, IEEE Electron Device Letters, Vol. 18, No. 2, February 1997.

[24] Dayal, A., Shrivastava, A. K., Vidyarthi, A, Akashe, S., “Nano-Scale Silicon MOSFETs: Modelling and Simulation Challenges in the Ballistic limit”, Emerging Research Areas and 2013 International Conferences on Microelectronics, Communications and Renewable Energy (AICERA/ICMICR)” 2013.